Journal of ELECTRONIC MATERIALS, Vol. 46, No. 5, 2017
DOI: 10.1007/s11664-016-5073-5

Fabrication of 200 mm Diameter Sintering Body of Skutterudite Thermoelectric Material by Spark Plasma Sintering

T. TOMIDA,[1,2] A. SUMIYOSHI,[1] G. NIE,[1] T. OCHI,[1] S. SUZUKI,[1] M. KIKUCHI,[1] K. MUKAIYAMA,[1] and J.Q. GUO[1]

1.—Thermoelectric Conversion Group, Tsukuba Development Center, Development Division, Furukawa Co., Ltd., 1-25-13 Kannondai, Tsukuba, Ibaraki 305-0856, Japan. 2.—e-mail: t-tomida@furukawakk.co.jp

Filled skutterudite is a promising material for thermoelectric power generation because its ZT value is relatively high. However, mass production of high-performance thermoelectric materials remains a challenge. This study focused on the sintering process of thermoelectric materials. Large-diameter *n*-type (Yb or La, Ca, Al, Ga, In)$_{0.8}$(Co, Fe)$_4$Sb$_{12}$ skutterudite sintering bodies with a small thickness were successfully produced by the spark plasma sintering (SPS) method. When direct current flows through the thermoelectric sintering body during the SPS pulse, the Peltier effect causes a temperature difference within the sintering body. To eliminate the Peltier effect, an electrical insulating material was inserted between the punch (electrode) and the sintering body. In this way, an *n*-type La-filled skutterudite sample with a diameter of 200 mm, thickness of 21 mm, and weight of 5 kg was successfully produced. The thermoelectric properties and microstructures of the sample were almost the same throughout the whole sintering body, and the dimensionless figure of merit reached 1.0 at 773 K.

Key words: Mass production, skutterudite, thermoelectric performance, spark plasma sintering

INTRODUCTION

Utilization of the large amount of thermal energy lost to the air as waste heat is a significant problem to be solved. Thermoelectric (TE) devices can directly convert thermal energy to electrical energy, thereby providing a way to effectively utilize waste heat. In addition, TE devices have no moving parts to cause noise or abrasion, so TE power generation systems are expected to offer long durability and high reliability.

Skutterudite materials are considered one of the best materials for power generation at intermediate temperatures owing to their promising TE properties.[1–3] The TE performance of a material is evaluated by the dimensionless figure-of-merit $ZT = TS^2/\rho\kappa$, where S is the Seebeck coefficient, ρ the electrical resistivity, κ the thermal conductivity, and T the absolute temperature. The larger the ZT value, the higher the energy conversion efficiency. Since Caillat et al.[1] reported excellent TE performance for skutterudites, these materials have attracted considerable attention as promising new TE materials. The skutterudite structure contains one large void in each cell. Filled skutterudites can be obtained by inserting heavy metal atoms into the voids. Because filling atoms can provide electrons, the optimum electron concentration can be obtained experimentally. Meanwhile, the filling atoms also act as phonon scattering centers to decrease the lattice thermal conductivity. Therefore, the ZT value of filled-skutterudite materials can be greatly improved.[4] Large ZT values have been reported in the literature[5–9] and we confirmed that the ZT values of *p*/*n*-type skutterudites reached *p*-ZT = 0.75 and *n*-ZT = 1.0,[8,9] and their TE performance did not degrade after annealing at 600°C for 5000 h under vacuum.[10]

(Received May 28, 2016; accepted October 18, 2016; published online November 3, 2016)

Compared to studies on the materials, research on mass production of TE materials, which poses a challenge, has been reported less frequently. Zheng et al.[11] recently reported the fabrication of large-size Bi_2Te_3-based ingots with diameters of 30 mm, 40 mm, and 60 mm, and they discussed the preparation of homogenous ingots. Here, we report another method to produce large sintering samples by spark plasma sintering (SPS).

EXPERIMENTAL PROCEDURES

Raw materials such as pure metals and/or alloys of n-type (Yb or La, Ca, Al, Ga, In)$_{0.8}$(Co, Fe)$_4$Sb$_{12}$ skutterudites were melted in crucibles at temperatures above 1000°C and then atomized into fine powders. X-ray diffraction analysis demonstrated that these fine powders were not a single skutterudite phase but a mixture of (Co, Fe)Sb_2, (Co, Fe)Sb, Sb and skutterudite. The atomized powders were further sintered into bodies with diameters of 30 mm (for lab scale samples) to 200 mm (for scaled up samples) by SPS at temperatures between 700°C and 750°C, pressures below 40 MPa, and holding times between 20 min and 60 min. Figure 1 shows the configuration of the SPS equipment used in this experiment. The sintering temperature was controlled by a thermocouple, which was set at the center of the upper carbon punch 25 mm away from its bottom side. The opposite position's temperature was measured at the lower carbon punch. The configuration is the same as that of commercial SPS equipment; there were no external heaters, and no specially shaped carbon dies or fiber-reinforced molds were used. In the setup shown in Fig. 1, mica was used as the electrical insulating material. This insulator was only used to fabricate thick sintering bodies, such as those with a thickness of 21 mm. The electrical insulating material layers can prevent the Peltier effect from occurring in the sintering body so that the temperature difference between the top and bottom sides of the sintering body can be kept as small as possible. Instead of mica, other electrical insulating materials such as Si_3N_4, Al_2O_3, and AlN can also prevent the Peltier effect.

The sintering bodies were cut into disks 10 mm in diameter and 1 mm in thickness and into prisms with dimensions of $2 \times 2 \times 15$ mm^3 to evaluate their TE performance. Measurements of their Seebeck coefficients and electrical resistivity were simultaneously carried out from room temperature to 600°C in a helium atmosphere with a ZEM-2 apparatus (ADVANCE RIKO, Inc.). The thermal diffusivity was evaluated by a laser flash method (TC-7000, ADVANCE RIKO, Inc.), and the specific heat capacity was measured with a differential scanning calorimeter. The dimensionless figure of merit (ZT) was calculated based on the above measurements. The microstructures of the samples were observed and analyzed by scanning electron microscopy (SEM).

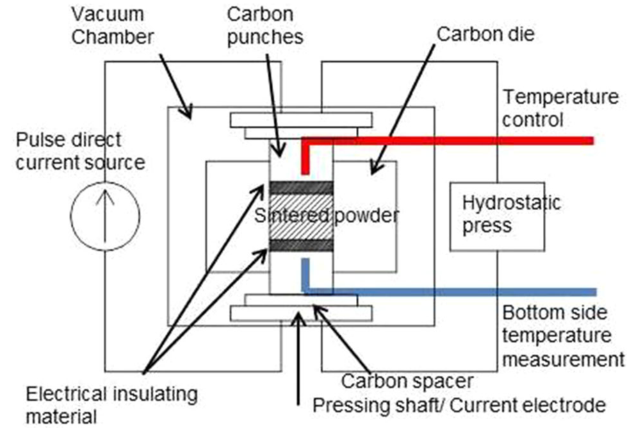

Fig. 1. Configuration of SPS equipment. The sintering temperature was controlled by a thermocouple, which was set at the center of the upper carbon punch 25 mm away from its bottom side. The opposite position's temperature was measured at the lower carbon punch.

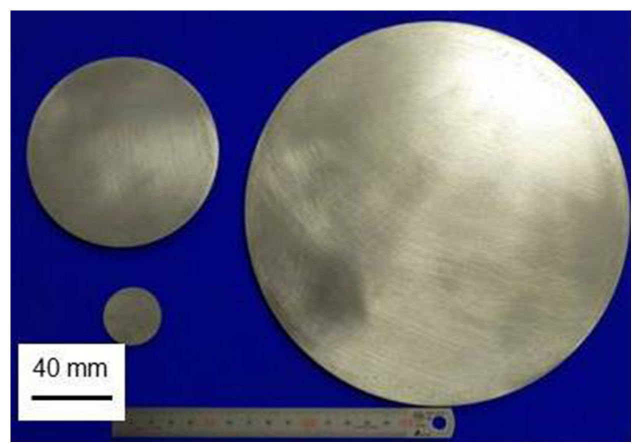

Fig. 2. Photograph of the Yb-filled skutterudite sintering bodies with diameters of 30 mm, 100 mm and 200 mm.

RESULTS AND DISCUSSION

Optimizing Fabrication Conditions of 200 mm Diameter Sintering Bodies Without Using an Insulator in SPS

The sintering conditions of 200 mm diameter sintering bodies were optimized using Yb- or La-filled skutterudites. Figure 2 shows the sintered samples of Yb-filled skutterudites with diameters of 30 mm, 100 mm, and 200 mm, which were fabricated under the optimized conditions for their respective diameters. No cracks or re-melting were observed in any of the samples.

The suitable sintering conditions at the lab scale for our n-type skutterudite materials were 700°C for 20 min. Sintering a 200 mm body under these conditions resulted in lower ZT value at the outer part of the sintered bodies due to their lower density in that region, which was caused by the low sintering temperature of the outer part. The densities of the inner and outer parts of 200 mm body

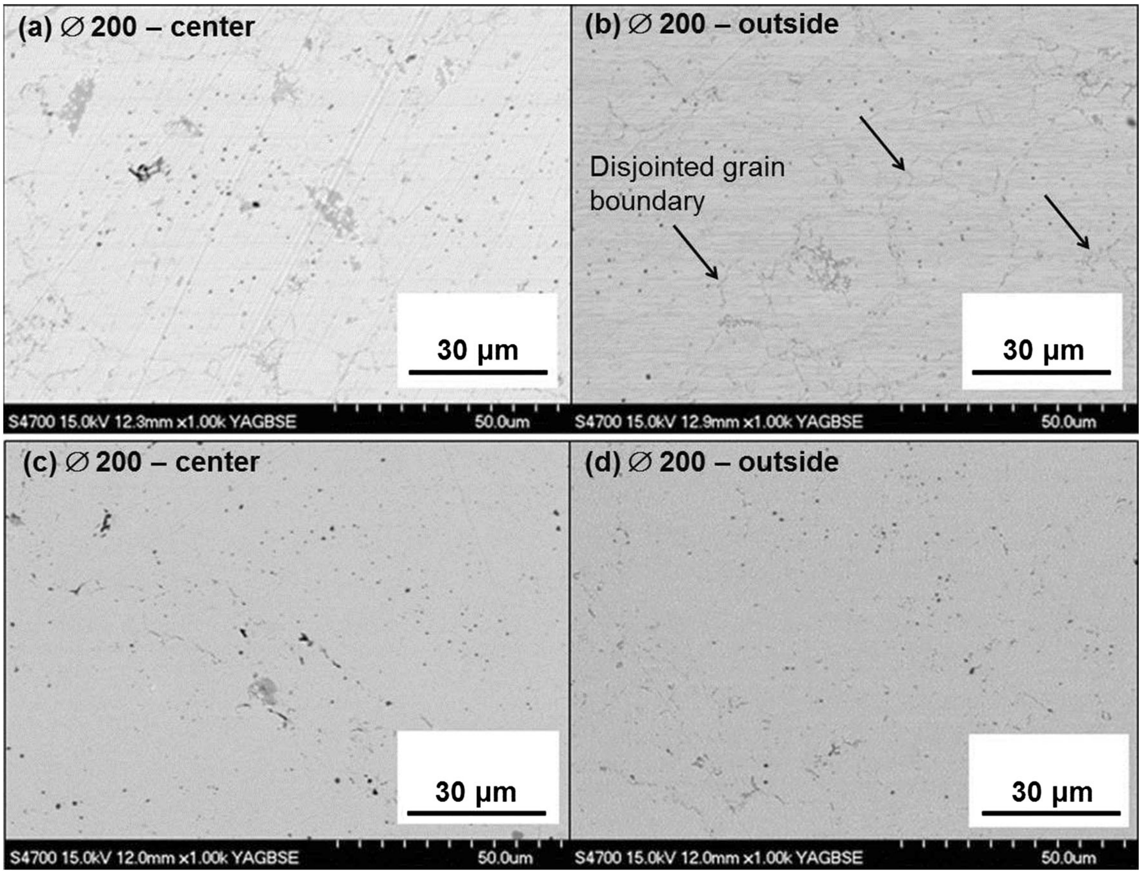

Fig. 3. Back scattering electron images of Yb-filled skutterudite sintering body with a diameter of 200 mm. (a) and (b) are the microstructures of non-homogeneous sintering body, (c) and (d) are those of homogeneous sintering body. The densities of (a)–(d) are 7.54 g cm^{-3}, 6.78 g cm^{-3}, 7.66 g cm^{-3}, and 7.67 g cm^{-3}, respectively. The marked areas show disjointed grain boundaries.

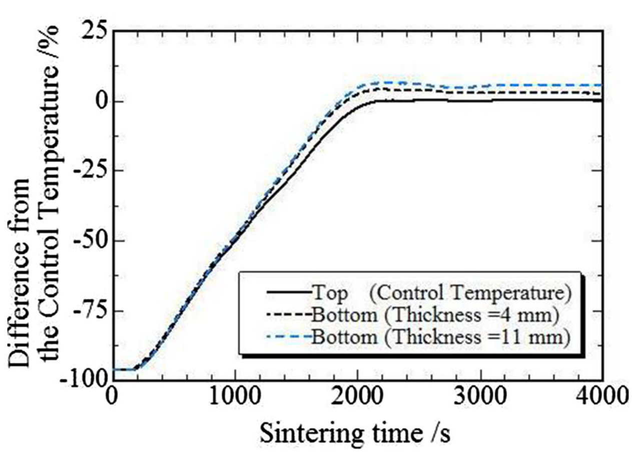

Fig. 4. The temperature difference between the top and bottom of the 200 mm diameter sintering body with thicknesses of 4 mm and 10 mm.

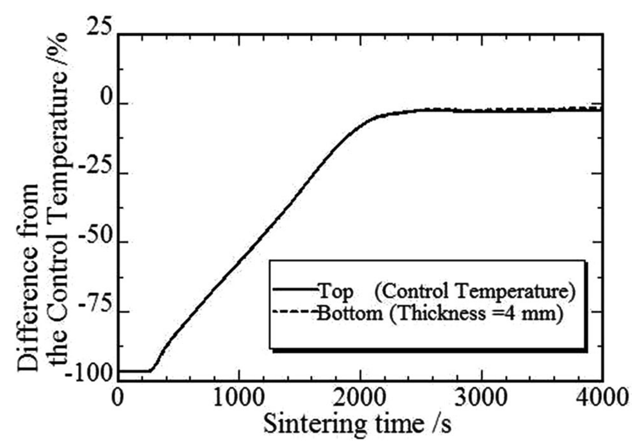

Fig. 5. The temperature difference between the top and bottom of the sintering body when the insulator was used.

were 7.54 g cm^{-3} and 6.78 g cm^{-3}, respectively. However, preparing 200 mm diameter sintering bodies under conditions similar to those of the small lab-scale sample is difficult. When the diameter of a sintering body becomes larger, so do the sintering dies. Because the heat capacity of a die increases with its size, the uniform heating conditions also change. Obtaining a high-density and homogeneous sintering body is critical for fabricating a 200 mm diameter sintering body. Taking into account the change in the heat capacity, the sintering temperature and time for the 200 mm diameter sintering body were selected to be 750°C and 60 min, respectively. Under these sintering conditions, the temperature difference between the center and outer part of the sintering body with a diameter of 200 mm and a thickness of 4 mm was less than 10°C, and uniform density and TE properties were obtained within the whole sintering body, resulting in ZT = 0.94.

The microstructures of these sintered samples were observed by backscattering electron microscopy. As shown in Fig. 3, when the sintering conditions were not proper, disjointed grain boundaries existed in the outer part of the 200 mm diameter sample. After the sintering conditions were optimized, the disjointed grain boundaries of the outer part decreased, and the density increased to 7.67 g cm^{-3}. This result is consistent with the relationship between the density and TE performance, i.e., the higher the density, the better the TE performance. For the Yb-filled skutterudite, we obtained a 200 mm diameter sintering body with a homogenous density, uniform TE properties, and ZT = 0.94.

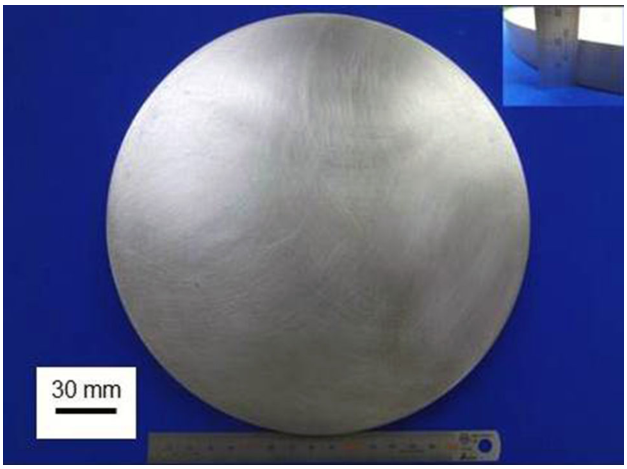

Fig. 6. Photograph of the La-filled skutterudite sintering body with a diameter of 200 mm, thickness of 21 mm and weight of 5 kg.

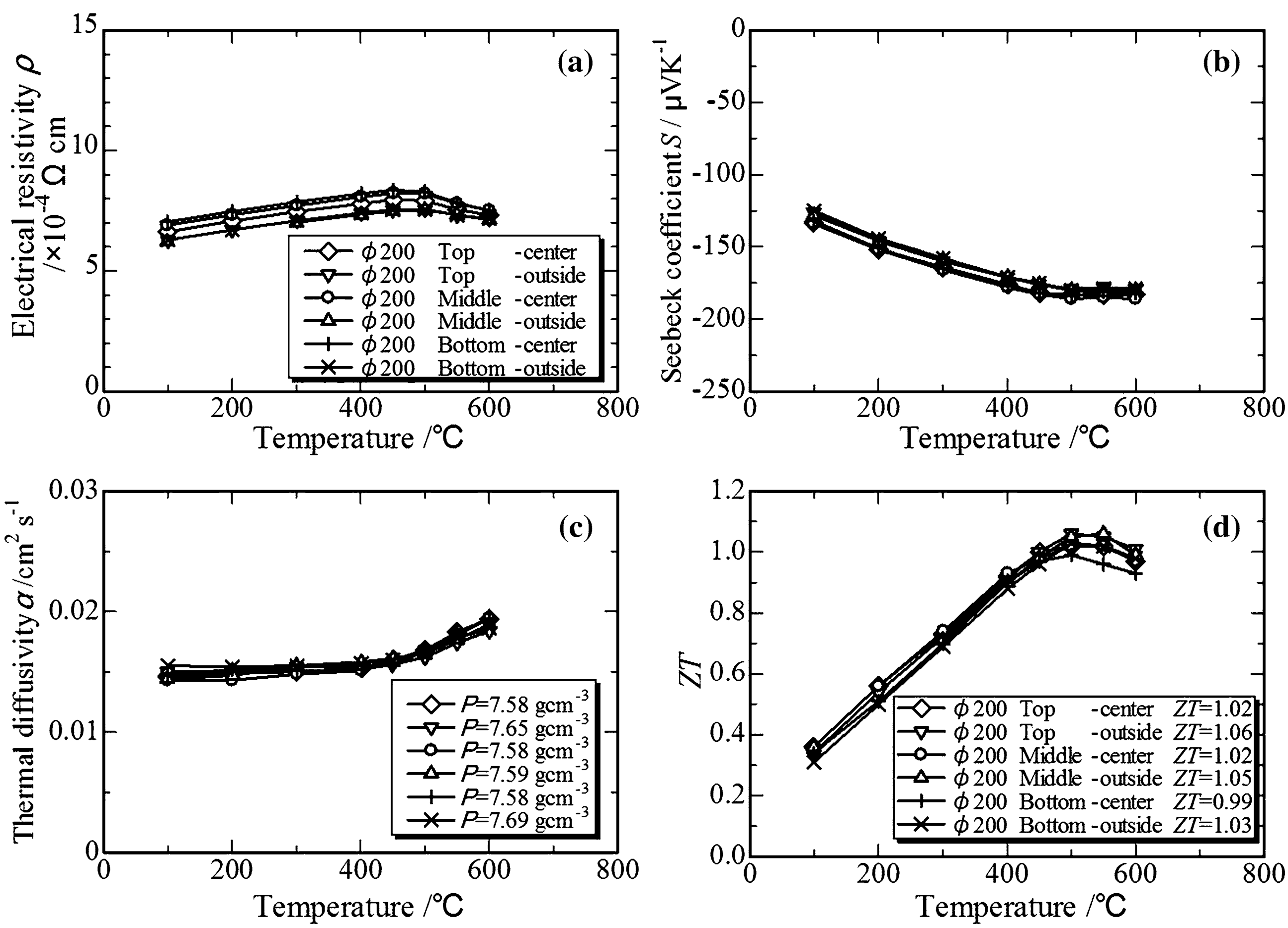

Fig. 7. The temperature dependence of (a) the electrical resistivity, (b) the Seebeck coefficient, (c) the thermal diffusivity and (d) ZT of the *n*-type La-filled skutterudite sintering body with the size of ∅200 − *t* 21 mm.

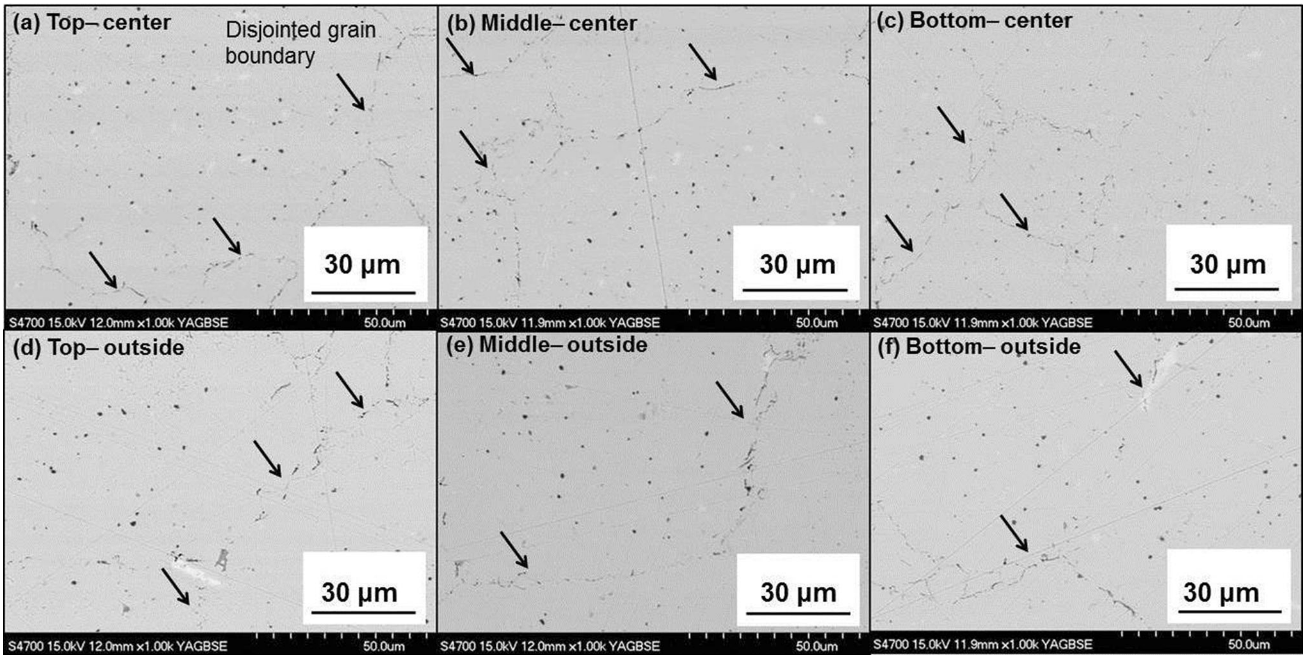

Fig. 8. Back scattering electron images of La-filled skutterudite sintering body with a diameter of 200 mm and thickness of 21 mm. The densities of (a)–(f) are 7.58 g cm^{-3}, 7.58 g cm^{-3}, 7.58 g cm^{-3}, 7.65 g cm^{-3}, 7.59 g cm^{-3}, and 7.69 g cm^{-3}, respectively. The marked areas show disjointed grain boundaries.

Further Scaling Up the Sintering Body Size Using an Insulator in SPS

For large-thickness sintering bodies, obtaining a homogenous TE performance within the sintering body is difficult. A temperature difference often exists between the top and bottom sides of the sintering body. Figure 4 shows the temperature difference between the top and bottom of the 200 mm diameter sintering body with thicknesses of 4 mm and 10 mm. The temperature difference increased with the thickness. When the thickness was as large as 20 mm, the temperature difference was too large to obtain a homogenous sintering body. On the other hand, during the sintering of a *p*-type material, this temperature difference was reversed. The temperature difference is caused by the Peltier effect when direct current flows through the TE sintering body during the SPS pulse. The better the TE performance of the sintering material, the larger would be the temperature difference. The Peltier effect during sintering of TE materials is an unavoidable problem for direct current SPS systems that is difficult to solve by changing only the sintering conditions. To eliminate the Peltier effect, thin layers of mica, an electrical insulating material, were inserted between the punch (electrode) and the sintering, body as shown in Fig. 1, so that the pulsed direct current could not flow directly through the TE sintering body. Figure 5 shows the temperature difference between the top and bottom of the sintering body when the insulator was used. The temperature difference between the top and bottom of the sintering body disappeared, indicating that the Peltier effect did not occur. At the same time, the pulsed direct current flowed mainly through the carbon dies, thereby heating the carbon dies first, which in turn heated the sintering body. Figure 6 shows a photograph of the La-filled skutterudite sintering body with a diameter of 200 mm, thickness of 21 mm and weight of 5 kg. The temperature dependence of the TE properties of the $\varnothing 200 - t$ 21 mm sintering body is shown in Fig. 7. The Seebeck coefficients, electrical resistivity, thermal diffusivity and ZT of the large-size sintering sample were almost the same within the whole sintering body, including at the center, outside, top, middle and bottom positions of the sintering body. The microstructure of the $\varnothing 200 - t$ 21 mm sintering body is shown in Fig. 8. The disjointed grain boundaries still existed within the sintering body. However, compared with Fig. 3b (the sample with inferior TE properties), the sintering body was denser, and there were fewer disjointed grain boundaries. These results indicate that the $\varnothing 200 - t$ 21 mm sintering body was homogeneously fabricated. Its ZT value reached 1.0.

CONCLUSIONS

Electrical insulation material layers were inserted at the interfaces between the punches (electrode) and the sintering body to prevent the Peltier effect, i.e., a temperature difference occurring between the top and bottom sides of the sintering body. In this way, an *n*-type La-filled skutterudite sample with a diameter of 200 mm, a thickness of 21 mm, and a weight of 5 kg was successfully fabricated by SPS. The TE properties and microstructures of the sample were almost the same throughout the whole sintering body, and the ZT value reached 1.0 at 773 K.

ACKNOWLEDGEMENTS

This research was supported by Future Pioneering Projects/Research and Development of Thermal Management Materials and Technology (TherMAT) of the New Energy and Industrial Technology Development Organization (NEDO) and the Japanese Ministry of Economy, Trade, and Industry.

REFERENCES

1. T. Caillat, J. Kulleck, A. Borshchevsky, and J.-P. Fleurial, *J. Appl. Phys.* 79, 8419 (1996).
2. G. Slack and V.G. Tsoukala, *J. Appl. Phys.* 76, 1665 (1994).
3. V. Keppens, D. Mandrus, B.C. Sales, B.C. Chakoumakos, P. Dai, R. Coldea, M.B. Maple, D.A. Gajewski, E.J. Freeman, and S. Bennington, *Nature* 395, 876 (1998).
4. B.C. Sales, D. Mandrus, B.C. Chakoumakos, V. Keppens, and J.R. Thompson, *Phys. Rev. B* 56, 15081 (1997).
5. X.F. Tang, Q. Zhang, L. Chen, T. Goto, and T. Hirai, *J. Appl. Phys.* 97, 093712 (2005).
6. J. Yu, W.Y. Zhao, X. Yang, P. Wei, D.G. Tang, and Q.J. Zhang, *J. Electron. Mater.* 41, 1395 (2012).
7. H. Li, X.F. Tang, Q. Zhang, and C. Uher, *Appl. Phys. Lett.* 94, 102114 (2009).
8. J.Q. Guo, H.Y. Geng, T. Ochi, S. Suzuki, M. Kikuchi, and S. Ito, *J. Electron. Mater.* 41, 1036 (2012).
9. H.Y. Geng, T. Ochi, S. Suzuki, M. Kikuchi, S. Ito, and J.Q. Guo, *J. Electron. Mater.* 42, 1999 (2013).
10. G. Nie, T. Ochi, S. Suzuki, M. Kikuchi, S. Ito, and J.Q. Guo, *J. Electron. Mater.* 43, 1752 (2014).
11. G. Zheng, X. Su, X. Li, T. Liang, H. Xie, X. She, Y. Yan, C. Uher, M.G. Kanatzidis, and X.F. Tang, *Adv. Energy Mater.* 6, 1600595 (2016).